WETLANDS, Vol. 24, No. 3, September 2004, pp. 701–710

NOTE

USE OF BALLOON AERIAL PHOTOGRAPHY FOR CLASSIFICATION OF KUSHIRO WETLAND VEGETATION, NORTHEASTERN JAPAN

Michiru Miyamoto[1], Kunihiko Yoshino[2], Toshihide Nagano[3], Tomoyasu Ishida[4], and Yohei Sato[5]

[1] *Japan Society for the Promotion Science Fellow, National Institute Environmental Studies*
16-2, Onogawa, Tsukuba, Ibaraki, 305-8573, Japan
E-mail: miyamoto.michiru@nies.go.jp

[2] *Institute of Policy and Planning Science, The University of Tsukuba*
1-1-1 Tennou-dai, Tsukuba, Ibaraki, 305-8573, Japan

[3] *Faculty of International Agricultural and Food Studies, Tokyo University of Agriculture*
1-1-1, Sakuragaoka, Setagaya, Tokyo 156-8502, Japan

[4] *Faculty of Agriculture, Utsunomiya University*
350, Minemachi, Utsunomiya, 321-8505, Japan

[5] *Graduate School of Agricultural and Life Sciences, The University of Tokyo*
Yayoi, Bunkyo-Ku, Tokyo, 113-8657, Japan

Abstract: Kushiro wetland in northeastern Japan is a Ramsar-designated wetland of international importance (1980) that is characterized by high biodiversity and spatial heterogeneity. These characteristics of the wetland also present innumerable challenges for mapping and monitoring such unique ecosystems. Recent advances in remote sensing technology have provided many sensors with different spatial and spectral scales and resolutions. However, they are still inadequate for mapping wetland vegetation at a large scale for various reasons, such as inadequate resolution and high costs. This study was designed to evaluate the potential of balloon aerial photography to acquire high resolution (15 cm pixel size) imagery for mapping wetland vegetation in the Akanuma marsh. We used a standard 28-mm non-metric camera (Nikon-F-801), which was mounted on helium-filled balloons operated by a remote radio-controlled system. By creating digital vegetation maps from visual interpretation of mosaicked photos, ten general types of vegetation and twenty-seven specific categories (species mixes) were successfully delineated. It was possible to classify small shrubs mixed with herbaceous plants; moss bogs with pools; dwarf shrubs with sedges; and moss with alpine plants. From this research, it seems that balloon aerial photography is a powerful tool for mapping temperate wetland vegetation, allowing classification of specific and typical vegetation types to the genus and species level.

Key Words: temperate wetland, vegetation mapping, balloon aerial photography, mosaicking, visual photo interpretation, Akanuma marsh, Kushiro wetland

INTRODUCTION

Intensive monitoring of environmental changes in wetlands is needed because wetland vegetation, such as peat mosses and alpine plant, can be diverse and highly fragile. Detecting changes in vegetation distribution enables us to perceive how the natural wetland environment functions under the influence of environmental changes (Yamagata 1999, Nakano et al. 2000). At the same time, it helps us in monitoring processes such as the disturbance dynamics, restoration, and invasive species.

Recently, remote sensing (spaceborne and airborne) has become a valuable technique to obtain wetland information such as land cover and vegetation mapping (Harvey and Hill 2001). Aerial photography has been used widely for wetland delineation (Scarpace et al. 1981, Jensen et al. 1984, Kadmon and Harari-Kremer 1999, Harvey and Hill 2001). The textural features and superior spatial resolution of aerial photography give us a very useful data source for detailed wetland mapping (Jennings et al.1992).

Traditional ground-mapping methods have been developed with the use of GIS and remote sensing techniques for wetland research (Barrette et al. 2000). Wetlands are often spatially characterized by steep ecological gradients with vegetation units narrower than the pixel size of current satellite sensors (Johnston and Barson 1993). Harvey and Hill (2001) reported that, although 10 m is sufficient spatial resolution to distinguish between different vegetation types, it is not adequate for identifying similar or specific vegetation types and resulted in misclassification of sedges and mixed grasses. For instance, Kadmon and Harari-Kremer (1999) cited only three vegetation classes (trees, shrubs, and dwarf shrubs) that could be identified at a spatial scale of 3 m by using black and white aerial photographs. Color infrared photos are still used for better identification of wetland boundary area covered by water, drainage patterns, separation of coniferous forest from deciduous, and classification of some understory components (Lyon 2001); however Vincent (1997) noted insufficiency for delineation of deciduous forests and shrubs during leaf-off conditions in wetlands. Many studies have revealed that it is difficult to acquire details about certain wetland species on a small scale due to inadequate resolution characteristics of some remote sensing data, all of which demands a new and innovative mapping technique for vegetation species. The use of small scale photography is primarily limited to the identification of plant communities with distinct spectral characteristics (Miyamoto et al. 2001). For instance, some recent high resolution remote sensing data such as IKONOS have also been inadequate in resolving the changes in vegetation that are attributed to the misty and changeable weather condition in the summer season in northeast Hokkaido. Remote sensing data had to be supported by field data in order to delineate vegetation at the species level (Juan et al. 2000).

Scale-independent remote sensing platforms such as kites and balloons will be required to monitor vegetation in inaccessible terrain and map them at the species level at large scales. Scale-independent platforms give added flexibility in modifying the spatial resolution and, therefore, permit vegetation mapping at species level on a large scale. For this study, we used balloons for mounting the 28-mm non-metric camera (Nikon-F-801). Balloon platforms were preferred, as they were cost effective, reusable, and could be used for exposing sensors on many landscapes, such as the Hokkaido wetlands, which is difficult to study using satellite data. Various studies in the past have used balloons at different altitudes, where the aims were primarily restricted to meteorological and atmospheric observations at various altitudes ranging from 10 to 40 km (e.g., Miller et al. 1992, Varotsos and Kondrat'ev 2001). In other studies, balloons were used to monitor dams and river basins (Koizumi et al. 1986) and mangrove forests (Nagano 1990) at low altitudes of 500 to 800 m; to monitor crops (Inoue and Morinaga 1995), sea ice (Derksen et al. 1997), soil and rocks (Davis and Annan 1989, Buerkert et al. 1996, Gerard et al. 1997, Friedli et al. 1998), oceans (Garrison and Katzberg 2000), insects (Weyman et al. 1995), and peat bogs (Aber and Aber 2001) at very low altitudes of 20 to 500 m. However, we believe that sensors and cameras mounted on balloon platforms were used in few case studies, particularly where the objective was to observe, monitor, and delineate wetlands at the species level. The major objective of our study was to evaluate the potential use of balloon aerial photographs for classifying and mapping wetland vegetation at the species level in very inaccessible terrains.

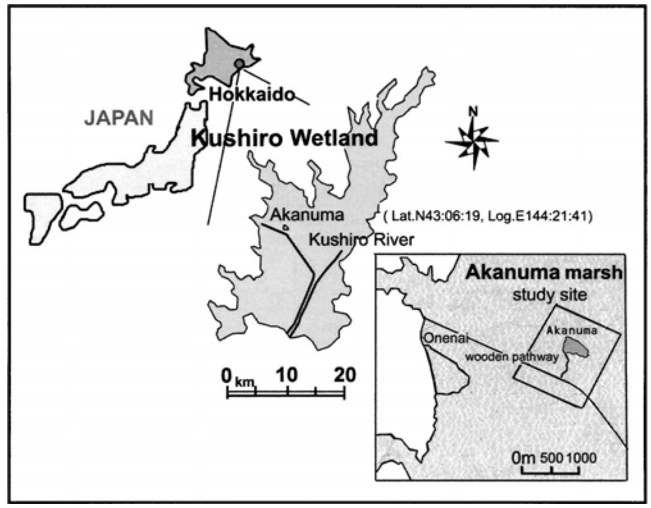

Figure 1. Study site, Akanuma marsh in Kushiro wetland (N 43:06:19, E 144:21:41), northeastern Japan.

STUDY AREA

The study site of Akanuma marsh is located in the Kushiro wetland (N 43°6′ 19″, E 144°21′ 23″) (Figure 1). Kushiro is the largest wetland in Japan, spreading over 18,290 ha and identified under the Ramsar convention (1980). It was designated as the first protected wetland in Japan. Topographically, the Akanuma marsh is flat with no slope, and the average elevation above sea level is 6 m (±20 cm). The mean annual temperature in Kushiro is 5.0 °C, which is the lowest recorded temperature of all the meteorological observations in Japan. Mean temperature of the coldest month (July) is 8.1 °C and the hottest month (August) 17.7°C. The mean annual rainfall is 1,200 mm and, due to the high density sea fog that forms from June to August (caused by Black and Oyashiro current flowing over Pacific Ocean), the duration of sunshine in summer time is short. These meteorological conditions

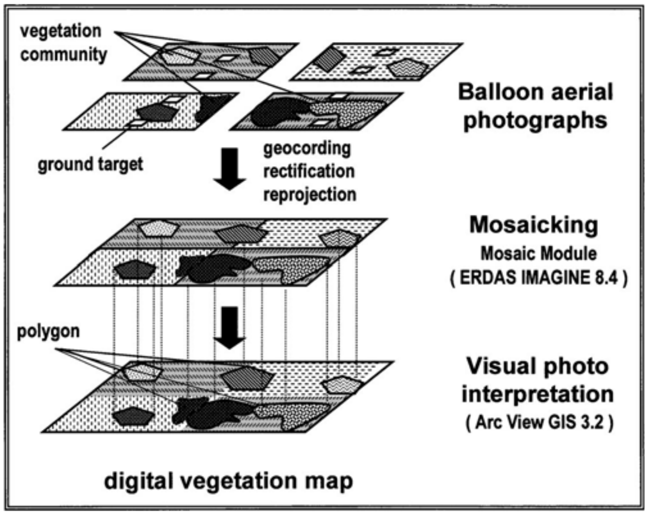

Figure 2. Process of digital vegetation mapping.

have given rise to this typical temperate wetland in northeast Japan (Honda 1993). Akanuma marsh is a designated protected area, characterized by high biodiversity and spatial heterogeneity of vegetation. Low moor dominate around Lake Akanuma, and transitional and high moors occur away from the lake. As broad categories, *Alunus japonica* (Thunberg) Steud. and *Phragmites australis* (Cavanilles) Trinius ex Steudel. dominate mainly in low-moor; *Myrica gale* var. *tomentosa* (C. DC.) Yamazaki and *Carex* spp. dominate in transitional moor; and *Sphagnum* bog, alpine plants, and dwarf shrubs dominate in high moor.

MATERIALS AND METHODS

The methodology involved the mapping of diverse vegetation at the species level in inaccessible terrain. An airborne platform consisting of two tethered, helium-filled balloons was used to mount the camera that was used to expose the vegetation belt in the study area. High-resolution, true color photographs were exposed at an altitude of 120 m and were mosaicked automatically by using the image analysis software ERDAS IMAGINE version 8.4 (Leica Inc.) A vegetation map was prepared by processing a mosaicked digital image with visual photo interpretation techniques. This process was used to classify wetland vegetation at the genus and species levels in order to monitor the vegetation of the study area.

The methodology was carried out in three main phases (Figure 2): 1) ground truthing and image data acquisition, 2) image calibration and mosaicking, and 3) visual photo interpretation and classification. In the first step, high resolution photographs were exposed over the study area, and the vegetation research was carried out for each wetland type. In the second phase, the photos were scanned, corrected for geometric distortions, and mosaicked into a seamless georeferenced image. Vegetation classes at the species level were delineated by using scientific visualization techniques. The base map was digitized and input into Arc View GIS (ver.3.2) software.

Table 1. GPS performance specifications.

Type: Integrated single frequency GPS survey unit, 4600 LS, Trimble Corp.
Standard features: RTCM version 2 input, NMEA-0183 output, internal memory
Size: 22.1 cm (Diameter) × 11.8 cm (Height)
Weight: 1.4 kg, 1.7 kg with batteries for >32 hours
Receiver power: <1 Watt receiver, 5 VDC with C-size batteries. 9 to 20 VDC external supply
Battery life: >32 hours continuous receiver operation on 4 standard C-size alkaline batteries
Static survey performance; Quick-Start, L1 Fast Static mode
Accuracy: ±5 mm + 1 ppm (≤10 km) (horizontal)
±10 mm +2 ppm (≤10 km) (vertical)
±1 arc second +5/baseline length in kilometers (azimuth)
Kinematic survey performance; Continuous, Stop-&-go mode
Accuracy: ±1 cm + 1 ppm (horizontal)
±2 cm + 1 ppm (vertical)
Occupation: 1 measurement (continuous),
2 epochs (min) with 5 satellites (Stop-&-go)

Vegetation Research and Position Coordinates

Vegetation research and position coordinates were determined by selecting ground control points (GCP). The vegetation research was conducted from June 30 to July 2, 1998 and from July 26 to 27, 2001 on the wooden path way in a North-South direction. Fifty-nine control points measuring 1m × 1m quadrats and fifty-two points measuring 10 m × 10 m quadrats were identified. Fifty-two points measuring 20 m × 20 m quadrats were identified in an East-West direction at an interval of 20 m each. At each quadrat, dominance and sociability were measured. The dominance is a relative ratio of vegetation cover of certain species in a unit area, whereas sociability is determined by the spread of species in a given area. Protected species that were listed by the National Environmental Agency were also identified. GPS measurements were recorded by positioning the instrument at the center of each ground target and the representative homogeneous vegetation type in each quadrat, respectively. The position coordinates were measured using two sets of ground-positioning systems (GPS, Trimble Corp., 4600LS) (Table 1) and by carrier phase Differential GPS. We placed twenty-one ground targets (30 cm × 30 cm) at 20-m intervals all along the wooden pathway, and ten ground targets (1 m × 1m) were placed

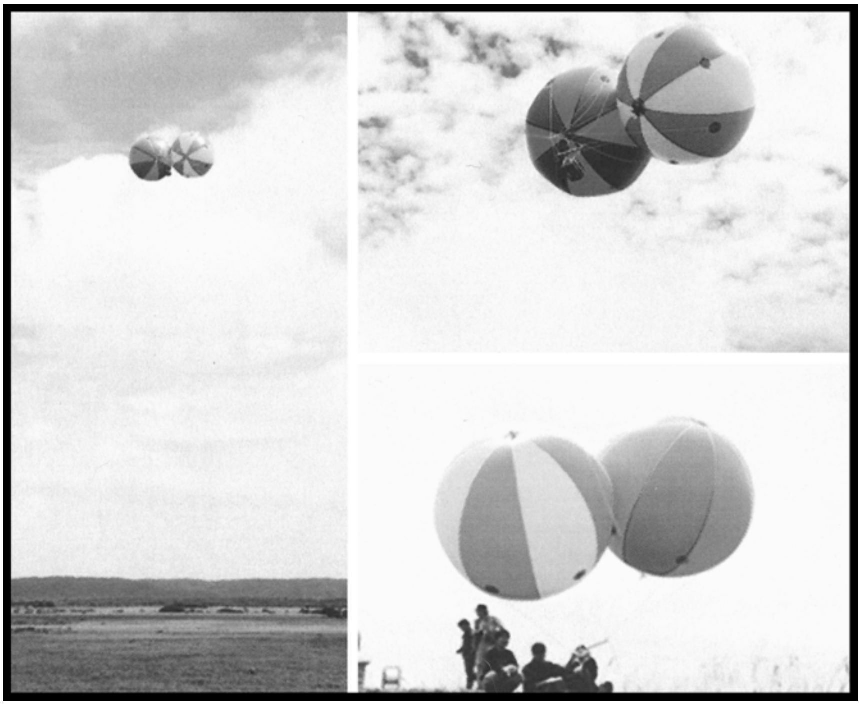

Figure 3. Snapshots of two tethered, helium-filled balloons.

on the footpace in Akanuma marsh from June 30 until July 2, 1998). These two ground targets were built of foam with plastic film and marked with a black cross. The GCPs were set on an embankment in Kushiro by a rapid static GPS survey process. The ground targets on the wooden pathway were measured in the kinematic mode. The position coordinates were converted to 13th plane rectangular coordinates using the data sets of electronic control points provided by the National Geographical Survey Institute, Japan. The tie points in the photographs were extracted by visual photo interpretation.

Table 2. Performance of tethered, helium-filled balloons.

Balloon type: spherical shaped balloon
Number of balloons: 2
Diameter/balloon: 2.4 m
Body material and thickness: polyvinyl chloride, 0.15 mm
Body weight: 2 kg × 2
Volume: 7 m^3 × 2
Helium supply: 7 m^3 × 2
Helium buoyancy: 69.6 N (Newton) × 2
Flight altitude above the ground: 120 m
Tether material: cotton and nylon
Tether diameter and weight: 6 mm (cotton) and 4 mm (nylon)
Tether weight: 55 g/m (cotton) and 0.01 kg/m (nylon)
Tether tension strength: 1000 N (Newton)
Sustainable flight duration: 48 hours
Actual flight duration/day: 4–5 hours
Field operation: manpower, 2 persons
Feasible weather: equable and mild weather with no wind
Suitable field condition: relatively flat ground
Helium cost/balloon: 300 USD × 2
Body cost/balloon: 500 USD × 2

Balloon System

Our remote sensing platform consisted of two tethered, helium-filled balloons and camera systems (Figure 3). In order to maintain the horizontal plane and equilibrium of the platform, two balloons were preferred instead of one. This lent stability to the platform and minimized tilt and related distortions. Aerial photo images were taken at an altitude of 120 m on July 2, 1998. The commercial spherical balloons (Table 2) (Figure 4) were made of a 0.15-mm polyvinyl chloride material that weighed 2 kg (per balloon) and were filled with 7 m^3 (per a balloon) of helium gas. With an air temperature of 18°C on the ground, the average lift for the balloons with tether and photographic equipment was approximately 139.2 N (Newton) with helium filling. The sixteen-legged, 6-mm cotton tethers (2m) attached to the balloons were fixed with an aluminum bar (1m), which carried the camera system. The captive tether of 4-mm nylon attached with a winch weighed 0.01 kg / m, and the strength of tension was 1000 N (Newton) (Nagano 1990). The total cost of helium gas was 600 USD, while the balloons bodies cost 1,000 USD.

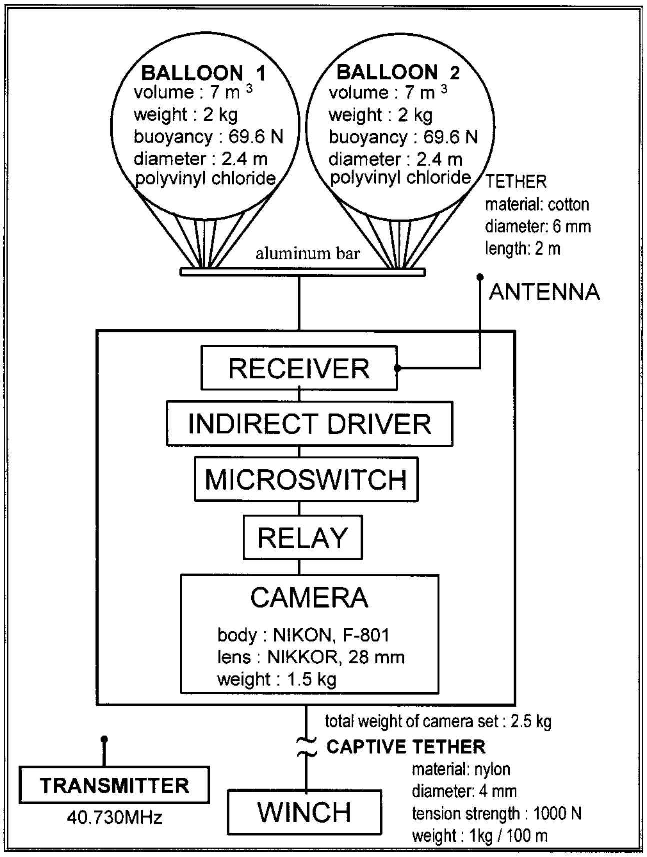

Figure 4. Schematic diagram of remotely-controlled, balloon-mounted aerial photography system.

Photographic Equipment and Remote Control

The photographic equipment consisted of both the standard 28-mm non-metric camera (Nikon F-801) and the radio-controlled system set (Table 3). The automatic shutter speed adjustment was radio-controlled by the transmitter (40.730 MHz). The camera body weight was 0.95 kg, while the total photographic equipment was 2.5 kg. The focal length of the camera was 28 mm (Nikkor f: 2.8), and the lens was covered by a filter (Kenko, SKY LIGHT). The receiver was connected with a relay switch to the micro switch and driver. The antenna wire was suspended horizontally along the balloon and vertically along the tether. The camera system has no special control to keep the camera in a perpendicular direction. However, Nagano (1990) noted that the higher the altitude, the more stable atmospheric conditions become. Photographs were taken along the wooden pathway between 6 and 11 AM to avoid the influence of wind and fog. Color negative film (35 mm) was used, and sixty-six shots were taken. Each photograph was 144 m (width) × 97 m (height). The total photo mosaicked area was 230 m (width) × 250 m (height).

Table 3. Specification of balloon aerial photography and performance of camera and lens.

Camera model: NIKON F-801
Lens: NIKKOR 28 mm f/2.8
Lens filter: KENKO SKY LIGHT B-1, 43 mm
Camera body weight: 0.95 kg
Total weight of camera set: 2.5 kg
Camera film: 35 mm color negative film
Field operation: radio control
Transmitter: 40.730 MHz
Coverage size/photo: 144 m (width) × 97 m (height)
Total mosaicked coverage area: 230 m (width) × 260 m (height)
Resolution: 15 cm/pixel (scanned at 600 dpi)
Number of available georeferenced scenes: 23/66 shots

Mosaicking Aerial Balloon Photographs

Each photograph was scanned at a reasonably high dpi (600). The resolution of the photographs was 15 cm × 15 cm / pixel. We took sixty-six sheets of photo images and the twenty-three sheets of photo images that were georeferenced and mosaicked using the MOSAIC module in ERDAS IMAGINE Ver.8.4 software (Leica Inc.) All photo images were georeferenced before mosaicking, and an image matching operation was applied in the overlap area (Figure 5). Contrast adjustment at the boundaries between photographs was carried out by automatically recalculating the pixel values for each photograph.

Visual Photo Interpretation and Construction of Digital Processed Vegetation Map

The mosaicked photo image was interpreted with the help of ground observations of plant species for every quadrat. Each vegetation community was delineated by visual photo interpretation to the genus and species levels. Polygons were manually digitized by the heads up digitizing technique using desktop Arc View GIS (ver.3.2) software. Polygons representing the same vegetation type were extracted and labeled based on the GPS and field study. A detailed vegetation map at the genus and species level was prepared.

RESULTS

The main aim of the study was to test the potential of alternate techniques such as balloon based remote sensing of vegetation, particularly in areas where satellite remote sensing and aircraft remote sensing approaches were inadequate. Although there are many sensors at different resolutions, balloon-based platforms are still important to map vegetation at the genus and species level. We successfully demonstrated the

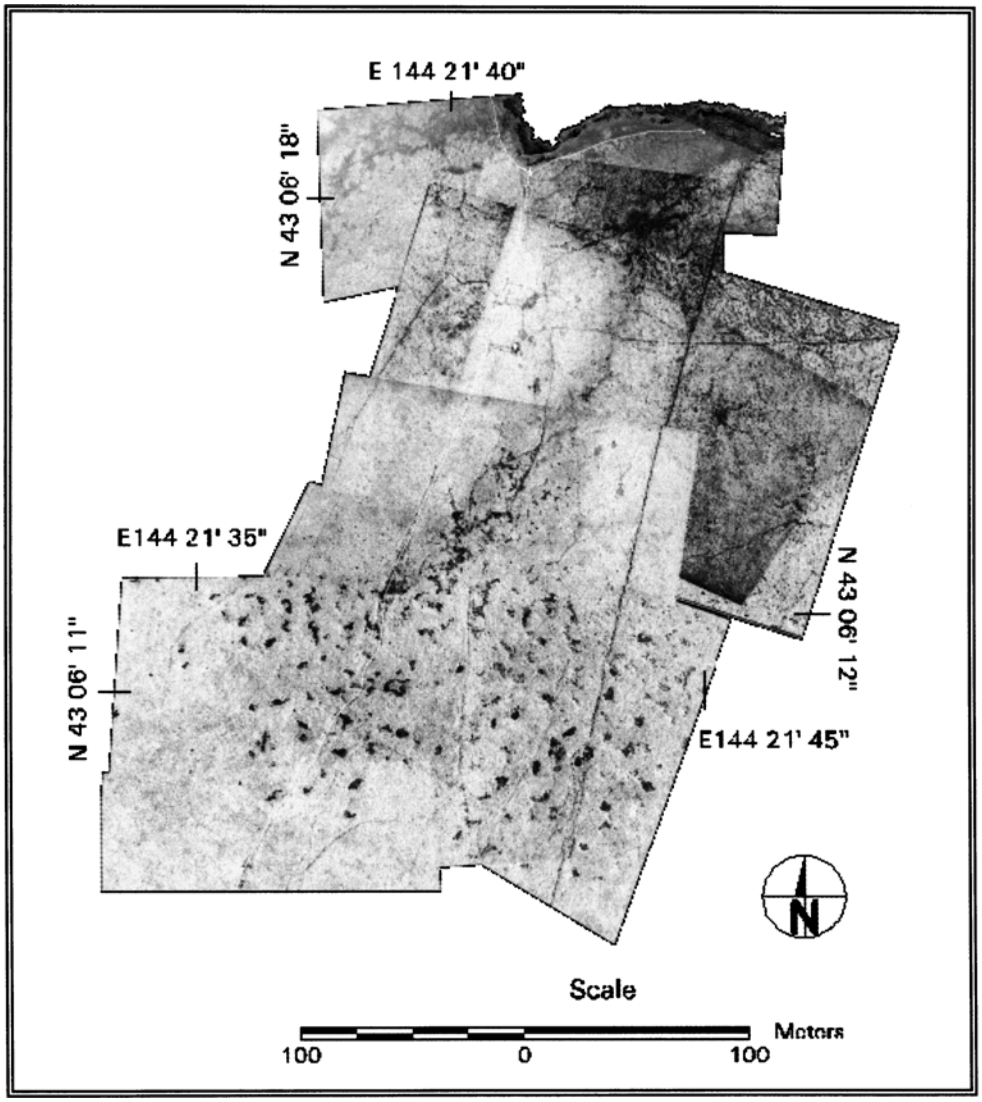

Figure 5. Mosaicked aerial balloon photograph at Akanuma marsh in Kushiro wetland. The twenty-three sheets of photographs were mosaicked by using MOSAIC module in ERDAS IMAGINE Ver.8.4 software (ERDAS).

effectiveness of this approach, which is required for large scale and detailed mapping in inaccessible terrain. Specifically, we achieved in the following.

Mosaicking of Aerial Balloon Photography

The contrast in each photograph was slightly different due to the difference in time when the photos were taken. Therefore, after the mosaicking process, the visual photo interpretation was done instead of automatic clustering process software. The misalignment occurred in the overlapping areas between two photographs. The actual error was 1.5 m. This error resulted from three factors: 1) ground targets could not be set in the marshland preserved area, so there were not enough ground targets, especially between two of the photographs; 2) photographic distortions were not removed; 3) the slight difference in the contrast failed to pick up the cross shaped mark in the ground targets.

Identification of Specific and Typical Wetland Vegetation

We identified fifty-eight species of vegetation by ground checks. Scientific visualization revealed ten community types and twenty-seven categories of mixed species, which were mapped by photointerpretation technique using Arc View GIS (ver.3.2) software (Figure 6a). These species were further sub-divided into five types and eleven categories of conservation species (Figure 6b). They are listed in the National Importance Conservation Species in Kushiro Wetland registered by National Environmental Agency in Japan. Figure 7 shows the vegetation types and in-

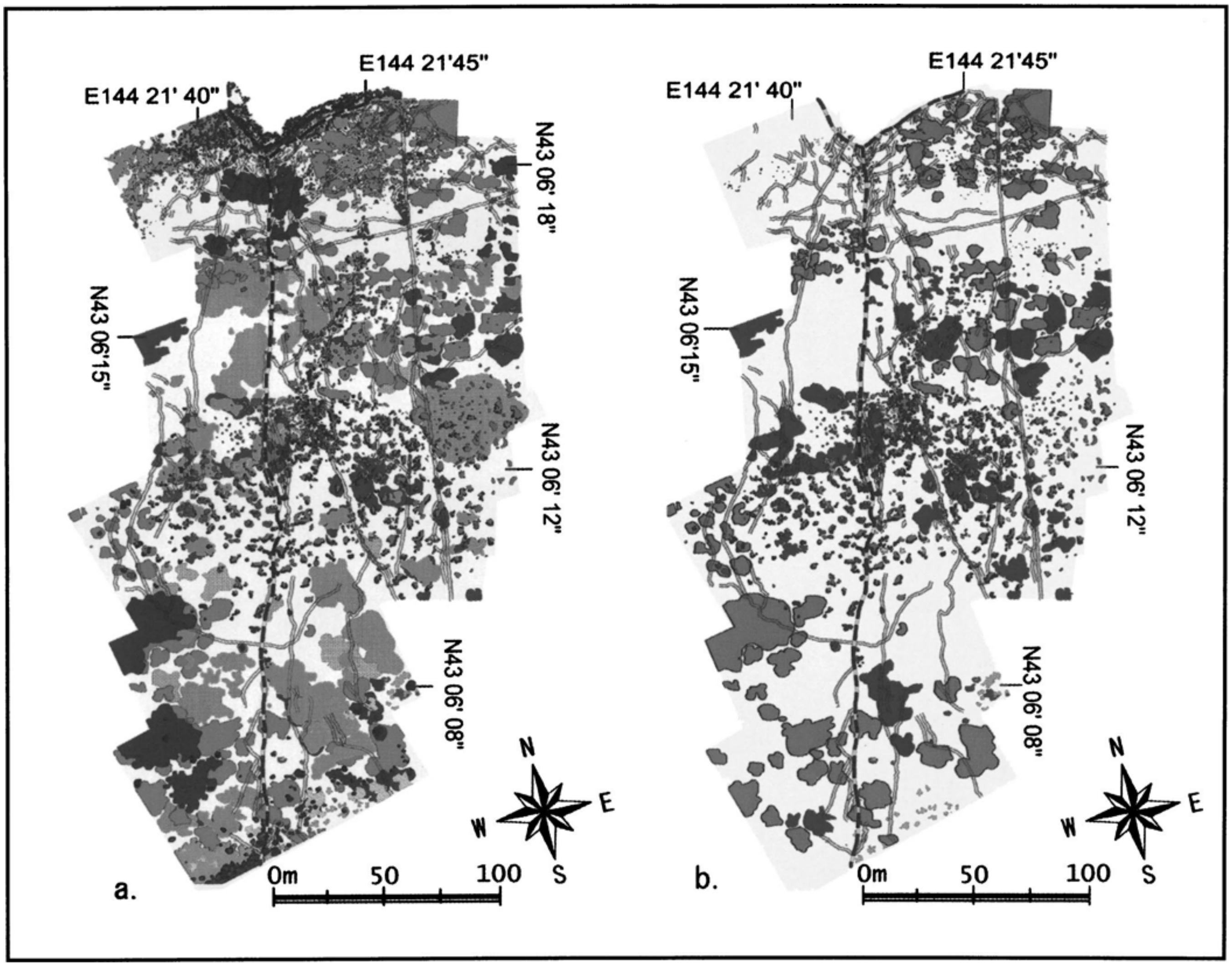

Figure 6. Final vegetation map (a) and conservation vegetation map (b) in Akanuma marsh in Kushir wetland. The conservation species are listed in the National Importance Conservation Species in Kushiro Wetland registered by National Environmental Agency in Japan.

dividual categories. The asterisks (*) represent the wetland conservation species. The vegetation types and individual categories are as follows: three types and seven individual categories in the low moor (1. aquiherbosa type, 2. shrub and herbaceous type, 3. herbaceous type); three types and six categories in the low-transitional moor (4. shrub, small shrub and herbaceous type, 5. small pool, small shrub, and herbaceous type, 6. small shrub and herbaceous type); one type and one category in the transitional moor (7. herbaceous type); three types and thirteen categories in the high moor (8. pool, moss, herbaceous, and alpine plant type, 9. moss and dwarf shrub type, 10. small pool with moss and herbaceous type). *Carex* spp. included *Carex lasiocarpa* Ehrhart var. *occultans* (Franch) Kukenth., *Carex pseudo curaica* Fr. Schm., *Carex middendoffii* Fr. Schm. We could discriminate the difference in the distribution in *Equiserum fluviatile* (*L.*), *Carex* spp. *and* aquiherbosa. These differences were represented by the darker green patches (coarse distribution) near the lake corresponding to waterlogged area and lighter green patches (dense distribution) away from the lake corresponding to high moor. In addition, the differences of the phenology of *Carex* spp.could be detected. These differences came from the darker brown patches (non-heads or forming heads) and light brown-pink patches (heads with flowers) in the transitional moor. The differences of vitality of *Phragmites australis* were represented by the brown-darker green patches (weak or deteriorated leaves, dominated in the dry inland away from the Akanuma pond) and the blue-green patches (vigorous

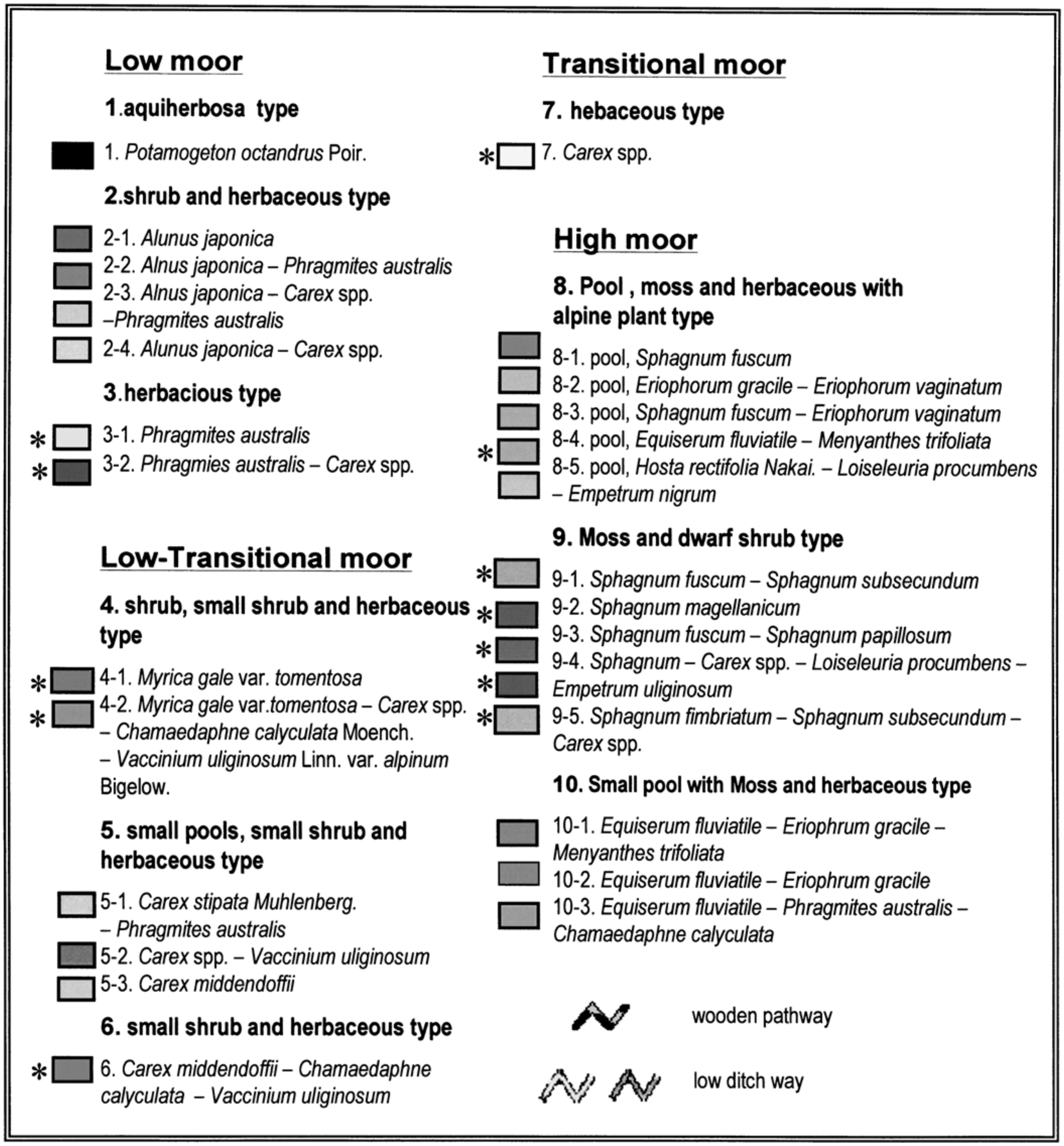

Figure 7. The legend of final vegetation map showing the ten types of specific vegetation and the twenty-seven of individual categories in each wetland type. The asterisks (*) represent the wetland preservation species.

leaves, dominated within 100 m of Akanuma pond). We clearly identified the four species of *Sphagnum* mosses, *Sphagnum fuscum* (Schimp.) Klinggr., *Sphagnum subsecundum* Nees ex Sturm., *Sphagnum magellanicum* Brid., *Sphagnum papillosum* Lindb. It was easy to distinguish among vegetation such as small shrubs mixed with herbaceous plants, moss bogs with pools, and dwarf shrubs with sedges, moss, and alpine plants. These data were compared and verified by ground checks.

DISCUSSION

Identification and mapping of wetland vegetation types at the species and genus level is important for sustainable management of wetlands that cannot be achieved using satellite and aircraft imagery. This is a special concern for delineating conservation species because they consist of perennial mixed species, small shrubs, alpine plants, and moss. In addition, monitoring changes of phenology and the health and biophysical status of the vitality in some perennial plants resulted in detailed classification. In an earlier study that used higher resolution IKONOS satellite data, we could not get clear imaging due to the typical fog in our study site. However, using balloon platforms, we could acquire cloudless aerial photographs for the site. In our study, we found mosaicked photography effective, not only for classifying vegetation up to species level, but also for monitoring change of phenology and condition status among green grasses and sedges. Balloon aerial photographs provide additional information necessary for detailed wetland classification. In addition, balloons are inexpensive and may be launched in most wetland study areas.

Regarding the performance of the balloon and camera system, distortion of the photography caused by the lens was found to be 4% near the edges around the corner as compared to the center of the photograph (Nagano 1990). When the camera is not exactly perpendicular, photographs are misaligned. In this experiment, photographs were almost always taken in no-wind conditions to avoid atmospheric influences. The distortion was not corrected since it was not a big problem in this experiment. Flight conditions were best between 6 and 11 AM, typically; however, they could be extended until 2 PM on cloudy days. The exact positioning of the balloon above a specific point typically required about 15 minutes. The flight altitude of 120 m was found to be suitable to identify vegetation patches to the species level.

Future technical developments should provide improvements in spectral measurement of physiological information and digital video images for easier acquisition of continuous mosaicked photos. Use of balloon platforms for monitoring terrestrial land cover is a basic remote sensing method; however, it is an effective technique for getting reliable information for detailed vegetation classification. These detailed maps will be necessary for conservation of biodiversity and spatial heterogeneity. Since wetlands have been and continue to be exposed to pressures from human activity, detailed wetlands classification will help us monitor disturbance dynamics, restoration, and invasive species. The simple mechanisms and ease of operation of balloon aerial photography may be useful for other ecological research, as well as vegetation monitoring.

ACKNOWLEDGMENTS

We are grateful to Mr. Toshitsugu Miyazaki in Kushiro Wetland Observation Visitor Center, Mr. Tatsuo Shibuya from Akkeshi Waterfowl Observation Center, and graduate students from University of Tsukuba and Hokkaido University. This research was partially funded by the Akkeshi town research fellowship and by the annual joint research project 2001 at the Institute of low temperature Science of Hokkaido University.

LITERATURE CITED

Aber, J. S. and W. S. Aber. 2001. Potential of kite aerial photography for peatland investigations with examples from Estonia. Suoseura 52:45–56.

Barrette, J., P. August, and F. Golet. 2000. Accuracy assessment of wetland boundary delineation using aerial photography and digital orthophotography. Photogrammetric Engineering and Remote Sensing 66:409–416.

Buerkert, A., F. Mahler, and H. Marschner. 1996. Soil productivity management and plant growth in the Sahel: potential of an aerial monitoring technique. Plant and Soil 180:29–38.

Davis, J. L. and A. P. Annan. 1989. Ground-penetrating radar for high-resolution mapping of soil and rock stratigraphy. Geophysical Prospecting 37:531–551.

Derksen, C., J. Piwowar, and E. Ledrew. 1997. Sea-ice melt-pond fraction as determined from low level aerial photographs. Arctic and Alpine Research 29:345–351.

Friedli, B., S. Tobias, and M. Fritsch. 1998. Quality assessment of restored soils: combination of classical soil science methods with ground penetrating radar and near infrared aerial Photography. Soil & Tillage Research 46:103–115.

Garrison, J. L. and S. J. Katzberg. 2000. The Application of Reflected GPS Signals to Ocean Remote Sensing. Remote Sensing of Environment 73:175–187.

Gerard, B., A. Buerkert, P. Hiernaux, and H. Marschner. 1997. Non-destructive measurement of plant growth and nitrogen status of pearl millet with low-altitude aerial photography. Plant and Soil 43:993–998.

Harvey, K. R. and G. J. E. Hill. 2001. Vegetation mapping of a tropical freshwater swamp in the Northern Territory, Australia: a comparison of aerial photographs, Landsat TM and SPOT satellite imagery. International Journal of Remote Sensing 22:2911–2925.

Honda, K. 1993. Kushiro Wetland, second edition. The Asahi Library, Asahi Shimbun, Tokyo, Japan.

Inoue, Y. and S. Morinaga. 1995. Estimating spatial-distribution of plant-growth in a soybean field-based on remotely-sensed spectral imagery measured with a balloon system. Japanese Journal of Crop Science 64:156–158.

Jennings, C. A., P. A. Vohs, and M. R. Dewey. 1992. Classification of wetland area along the upper Mississippi River with aerial videography. Wetlands 12:163–170.

Jensen, J. R., E. J. Christensen, and R. Sharits. 1984. National wetland mapping in South Carolina using airborne multispectral scanner data. Remote Sensing of Environment 16:1–12.

Johnston, R. M. and M. M. Barson. 1993. Remote sensing of Australian wetlands: an evaluation of Landsat TM data for inventory and classification. Australian Journal of Marine and Freshwater Research 44:223–232.

Juan, C., J. D. Jordan, and C. Tan. 2000. Application of airborne hyperspectral imaging in wetland delineation. Proceedings of The 21st Asian Conference on Remote Sensing, Taipei, Taiwan 2:834–839.

Kadmon, R. and R. Harari-Kremer. 1999. Studying long-term vegetation dynamics using Digital Processing of Historical Aerial Photographs. Remote Sensing of Environment 68:164–176.

Koizumi, T., M. Murai, T. Koike, and H. Manabe. 1986. An Automated System and its Application for Aerial Photography Using Kite Balloon. Journal of The Japan Society of Photogrammetry and Remote Sensing 25:12–23.

Lyon, J. G. 2001. Wetland Landscape Characterization: GIS, Remote Sensing, and Image Analysis, first edition. Ann Arbor Press, Chelsea, MI, USA.

Miller, S., M. Birk, F. Schreier, and D. Hausamann. 1992. Airborne far-infrared heterodyne remote-sensing of stratospheric OH-A feasibility study. International Journal of Infrared and Millimeter Waves 13:1241–1268.

Miyamoto, M., Y. Yoshino, and K. Kushida. 2001. Relationship between canopy BRDF and physical parameters of 3D structure of vegetation in northern wetlands in Japan. Asian Journal of Geoinformatics 1:57–70.

Nagano, T. 1990. Studies on mangrove in Thailand—an aerial photographic survey using a kite balloon. Japanese Society of Environment Control in Biology 28:119–124.

Nakano, T., S. Kuniyoshi, and M. Fukuda. 2000. Temporal variation in methane emission from tundra wetlands in a permafrost area, northeastern Siberia. Atmospheric Environment 34:1205–1213.

Scarpace, F. L., B. K. Quirk, R. W. Keifer, and S. L. Wynn. 1981. Wetland mapping from digitized aerial photography. Photogrametric Engineering and Remote Sensing 47:829–838.

Varotsos, C. A. and K. Y. Kondrat'ev. 2001. Experiment in integrated interpretation of remote sensing data and direct measurements of atmospheric ozone content. Earth Observation and Remote Sensing 16:511–526.

Vincent, R. K. 1997. Fundamentals of Geological and Environmental Remote Sensing, first edition. Prentice Hall, Upper Saddle River, NJ, USA.

Weyman, G. S., P. C. Jepson, and K. D. Sundreland. 1995. Do seasonal-changes in numbers of aerially dispersing spiders reflect population-density on the ground or variation in ballooning motivation. Oecologia 101:487–493.

Yamagata, Y. 1999. Advanced remote sensing technique for monitoring complex ecosystems: spectral indices unmixing and classification of wetlands. National Institute for Environmental Studies, Tsukuba, Japan. R-141.

Manuscript received 8 February 2002; revisions received 9 October 2002 and 31 February 2004; accepted 24 May 2004.